PCCP

Phase Transition in Amphiphilic Poly(N-isopropylacrylamide): Controlled Gelation

Journal:	*Physical Chemistry Chemical Physics*
Manuscript ID	CP-ART-03-2018-001609.R1
Article Type:	Paper
Date Submitted by the Author:	17-Apr-2018
Complete List of Authors:	Li, Bin; University of Southern California, Department of Chemistry Thompson, Mark; University of Southern California, Department of Chemistry

Phase Transition in Amphiphilic Poly(*N*-isopropylacrylamide): Controlled Gelation

Bin Li,[†] and Mark E. Thompson[*,†,‡]

[†]Department of Chemistry and [‡]Mork Family Department of Chemical Engineering and Materials Science, University of Southern California, Los Angeles, California 90089, United States

*E-mail: met@usc.edu.

for Table of Contents use only

Amphiphilic random poly(*N*-isopropylacrylamide) copolymers are found to form a hydrogel which is highly elastic, stable, thermo-reversible and self-healable.

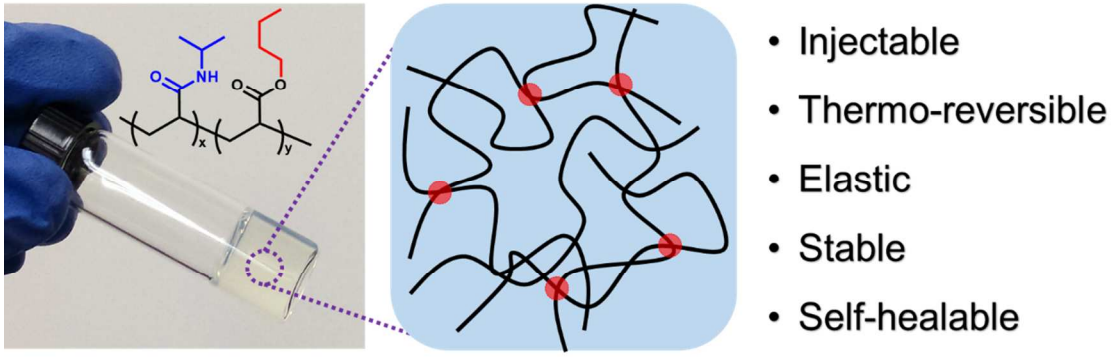

ABSTRACT:

Thermally reversible gelation of polymers is of converging interest in both the fundamental research and practical biomedical or pharmaceutical applications. While the block structure is widely reported to favor gelation, there are few studies regarding the behavior of amphiphilic random copolymers. Herein, hydrophobically modified poly(*N*-isopropylacrylamide) (pNIPAM) polymers were designed and synthesized by reversible addition-fragmentation chain transfer (RAFT) copolymerization of NIPAM and butyl acrylate (BA). A library of polymer systems was created by varying the BA: NIPAM ratio, molecular weight(Mw) and concentrations. While a coil-to-globule transition induced microphase separation occurred in the dilute solution, diverse phase behaviors were observed by phase diagram study. A transparent gel phase was identified in p(NIPAM-co-BA) systems, which was missing in its block counterpart pNIPAM-b-pBA, and existed over a wider temperature range with increased BA content, Mw and concentrations. A dynamic rheological analysis revealed that the gel properties were strongly dependent on temperature, which regulated the interchain hydrophobic association, and the gel proved to be highly elastic, stable, reversible and self-healable under the optimized conditions. The p(NIPAM-co-BA) system will be highly desirable for injectable in situ forming hydrogel materials, and the study demonstrated here can be potentially extended to other amphiphilic pNIPAM copolymers.

INTRODUCTION

Physically cross-linked hydrogels refer to networks held together by non-covalent associations, such as ionic, hydrogen-bonding, host-guest, metal-ligand and hydrophobic interactions.[1] Different from chemical crosslinking formed by covalent bonding between polymer chains, these physical interactions show dynamic behavior through the breaking and re-

formation of non-covalent linkages. The combined physical and chemical cross-linking endow the polymer system with reversibility, stimuli responsiveness, self-healing, and superior mechanical performance. [2, 3]

As a main driving force in guiding protein folding and polymeric self-assembly, [4] hydrophobic association has been reported as the cross-linking unit in building stable hydrogels, mostly found in synthetic block copolymers and modified biopolymers. [5] A micellar model has been proposed for hydrophobically associated hydrogels, and the aggregation of hydrophobic units into micelle cores contribute to the gel formation, presumably acting as the cross-linking sites. Increasing the length of the hydrophobic micelle-forming chains favors the gelation, and this accounts for the gelation mechanism of various amphiphilic block copolymers.[5-7] Theoretically, an appropriate hydrophobic-hydrophilic balance in amphiphilic copolymers could form hydrophobic domains surrounded by hydrophilic polymer segments, and further induce gelation if interpolymer interactions are dominant, even in random copolymers. The concept has been reported recently for copolymers of a hydrophilic monomer with a small amount of a hydrophobic comonomer, prepared via a micellar polymerization technique. [8, 9]

Poly(*N*-isopropylacrylamide) (pNIPAM) is a popular thermo-responsive polymer, and shows a coil-to-globule transition above its lower critical solution temperature (LCST). The corresponding phase separation is ascribed to the switch from a dominantly pNIPAM-water hydrogen bonding to entropy-driven hydrophobic association.[10] While dilute solutions above LCST yield aggregates with a few pNIPAM chains, more concentrated solutions form colloidal sized particles or macroscopic precipitates. Many pNIPAM based hydrogels have been developed incorporating additional chemical cross-linkers, but a thermo-sensitive sol-gel

transition of pNIPAM has only been observed for polymers with very high molecular weight (~10^6 g mol^{-1}) or isotactic-rich pNIPAM. [11, 12]

To promote the gelation of pNIPAM, the copolymerization with hydrophobic monomers can be an efficient method by enhancing the hydrophobic association and stabilizing the interpolymer interaction. Over the last two decades there have been sporadic reports of this phase transition for these copolymers in the semidilute range. [13-15] It is generally recognized that the hydrophobically modified pNIPAM shows broadened temperature range over which the phase transition is observed and enriched phase patterns, but the phase behavior varies among different reports,[14, 15] and remains to be investigated in detail.

Here we report a study on the phase behavior of a random copolymer of NIPAM and a moderately hydrophobic monomer, butyl acrylate (BA). Several important issues are addressed to yield a detailed phase map of hydrophobically modified pNIPAM. In contrast to a monomer with long alkyl chain previously used (e.g., dodecyl and octadecyl), the reactivity ratio of BA and NIPAM is similar due to the reduced steric hindrance, and a more statistical copolymer would be expected. The molecular weight distributions play a critical role in the phase transition of amphiphilic pNIPAM, and reversible addition-fragmentation chain transfer (RAFT) polymerization is employed to accurately control the molecular weight and polydispersity. A performance comparison of the polymer at different phase states, which includes reversibility and stability, is often missing in the literatures, and it will be emphasized in this study by rheological analysis.

EXPERIMENTAL SECTION

Materials. 2,2′ -Azobis(2-methylpropionitrile) (AIBN, 99%), *N*-isopropylacrylamide (NIPAM, ≥ 99%), butyl acrylate (BA, ≥ 99%), 4-cyano-4-[(dodecylsulfanylthiocarbonyl) sulfanyl] pentanoic acid (DCT, 97%) were purchased from Sigma-Aldrich and used without further purification. All solvents were reagent grade and used as such unless otherwise specified. The p(NIPAM-co-BA) copolymers will be abbreviated as P_x(Y), where x denotes the feed molar ratio percentage of BA to NIPAM, and Y refers to the number average molecular weight (Mn) in g mol^{-1} determined by GPC.

Polymer Synthesis. p(NIPAM-co-BA) copolymers were prepared using RAFT polymerization. Here we will illustrate the procedure used for all of the polymerizations with the one for P_5(19K). A mixture of NIPAM (2.00 g, 17.7 mmol), DCT (27 mg, 67 μmol) and AIBN (2.2 mg, 13 μmol; [DCT]: [AIBN]=5:1) was placed in a flask, 0.13 ml of BA (110 mg, 0.86 mmol) and 10 ml of dioxane were introduced into the flask through a syringe. The flask was then sealed, and the solution was purged with nitrogen for 30 min. The polymerization was conducted at 70 °C under a nitrogen atmosphere for 12 h. Afterwards, the polymerization was stopped by exposure to air and cooling to room temperature. The reaction mixture was diluted with acetone, precipitated in a large excess of hexanes and isolated by filtration. The isolated product was dried overnight under vacuum. The molecular weight of the polymer was controlled by DCT: NIPAM ratio (see Table 1).

The P_0 polymers were prepared by the same procedure as described for P_5, but the BA was left out of the synthesis. The P_{10} copolymers were prepared by this procedure with the addition of 10 mol% BA relative to NIPAM. Table 1 gives the properties of the P_0 and P_{10} copolymers used in our study.

The aqueous polymer solutions were prepared by dissolving various amounts of the polymers in deionized water which were kept in a refrigerator at ~4 °C for 1 week with occasional shaking. These solutions were then stored at 4 °C for another week to equilibrate and remove air bubbles.

Characterization. Fourier transform infrared (FTIR) spectrum was recorded on a Bruker Vertex 80 spectrometer over the wavenumber range of 500-4000 cm^{-1}. The polymer sample used in FTIR analysis was prepared using the KBr pellet method. ^{1}H NMR measurements were performed with a Varian VNMRS 600 MHz spectrometer, $CDCl_3$ was used as the solvent and the solvent signal was used for internal calibration. The gel permeation chromatography (GPC) measurements were carried out on a Waters GPC instrument equipped with four Waters Styragel columns (Styragel HR1, HR4, HR4E, and HR5E) and a refractive index detector. THF was used as the eluent at a flow rate of 1 mL min^{-1} at 35 °C. Relative molecular weights were calibrated with polystyrene standards. The temperature dependence of the particle size in polymer solution (5 mg mL^{-1} in DI water) was evaluated using dynamic light scattering (DLS, DynaPro Plate Reader II, Wyatt Technology). 0.2 °C min^{-1} heating rate was used with 5 min of thermal equilibration before data acquisitions at each temperature, both the light scattering intensities and hydrodynamic diameters of the polymers were plotted versus temperature, and the LCST was taken as the onset of the increase in light scattering intensity.[16]

Phase Transition. The phase transition of the aqueous polymer solution was examined using a vial tilting method as a function of temperature. The copolymer solutions with different concentrations (5, 10, 20 and 30 wt%) were prepared in a glass vial, and kept in a refrigerator prior to the experiment. The experiment was carried out in a thermostated water bath from 2 °C to 40 °C at 1 °C intervals, and at each temperature the samples were equilibrated for 5 min

before visual observation. The opaque state was identified with no background being visible, the gel phase was determined by tilting the vial when no fluidity was visually observed after 1 min, and the dehydrated state was recognized with water release observed with the naked eye.

Rheological Characterization. All rheological characterizations were performed on a TA Instruments DHR-2 equipped with a Peltier plate and a solvent trap to minimize water evaporation. A 20 mm diameter parallel plate geometry was employed with 0.5 mm gap. The linear viscoelastic region (LVR) for each sample was first determined using a strain sweep from γ= 0.01% to 1000% at constant temperature and constant frequency of 6.3 rad·s^{-1}. Frequency sweep was obtained at a strain amplitude of 0.5% over a frequency range of 0.05-100 rad·s^{-1}. A 1% strain within the LVR and a constant frequency of 6.3 rad·s^{-1} were applied in all the following rheological measurements. An oscillation temperature ramp was conducted from 10 °C to 50 °C with a heating rate of 1 °C min^{-1}, the gelation temperature (T_{gel}) was determined as the crossover point of storage modulus (G') and loss modulus (G"), and the temperature range with G'>G'' was defined as the gel region. Time dependence of the viscoelastic properties at different phase states was determined by monitoring G' and G" as a function of time. The thermo-reversibility of the polymer was conducted using an oscillation time sweep at two different temperatures that fell into different phase states. The duration time was 200 s for each temperature, and the temperature change was successively performed without a time interval. The thermal hysteresis was determined by measuring G' and G" during heating and cooling cycle between different phase states.

Self-healing Capabilities. Rheological failure-recovery study was conducted as time sweep at alternate step strains. Oscillatory time sweep was initially performed for 200 s with constant strain (1%) at its linear viscoelastic regime, followed by an oscillatory time sweep measurement

at 1000% strain for 50 s where the gel network was disrupted. After a resting step of 120 s, the shear strain was returned to 1%, and four failure-recovery cycles were applied consecutively. All measurements were performed at constant temperature (18 °C) and constant frequency (6.3 rad·s^{-1}).

For macroscopic self-healing observation, two hydrogel sheets were prepared in a round shape with one stained with rhodamine B to facilitate visualization. After cutting the gel into two pieces, they were put together in close contact, healing proceeded without any external intervention at constant temperature (18 °C), and photographs were taken at different time intervals to record the self-healing process of the hydrogel.

RESULTS AND DISCUSSION

Characterization and Solution Properties of P(NIPAM-co-BA)

The preparation of p(NIPAM-co-BA) was accomplished by RAFT copolymerization of NIPAM and BA with the aid of a chain-transfer agent, 4-cyano-4-[(dodecylsulfanylthiocarbonyl) sulfanyl] pentanoic acid (DCT), which gave good control of the copolymer structure (Scheme 1).[17, 18] Both of the monomers were successfully incorporated into the polymer chains, with all the signals identified in its FTIR and ^{1}H NMR spectra. The controlled nature of the RAFT polymerization was demonstrated by the unimodal and narrow peak in GPC trace (see SI). At a constant feed ratio of two monomers, the polymer steadily shifted to a higher molecular weight (Mw) with an increased monomer to DCT ratio. At a fixed monomer to DCT ratio, the polymer maintained the similar Mw using a BA: NIPAM molar ratio of 0:100, 5:100 and 10:100. All the polymers showed low polydispersity (1.16-1.38, Table 1), which allowed the examination of molecular weight and BA: NIPAM ratio effect on the phase transition behavior. The p(NIPAM-co-BA) copolymers will be abbreviated as P_x(Y), where x denotes the feed molar ratio of BA to

NIPAM, and Y refers to the number average molecular weight (Mn) in g mol^{-1} determined by GPC. For example, a polymer that has BA present in a 5% molar ratio and has a molecular weight of 19,400 g mol^{-1} will be abbreviated P_5(19K).

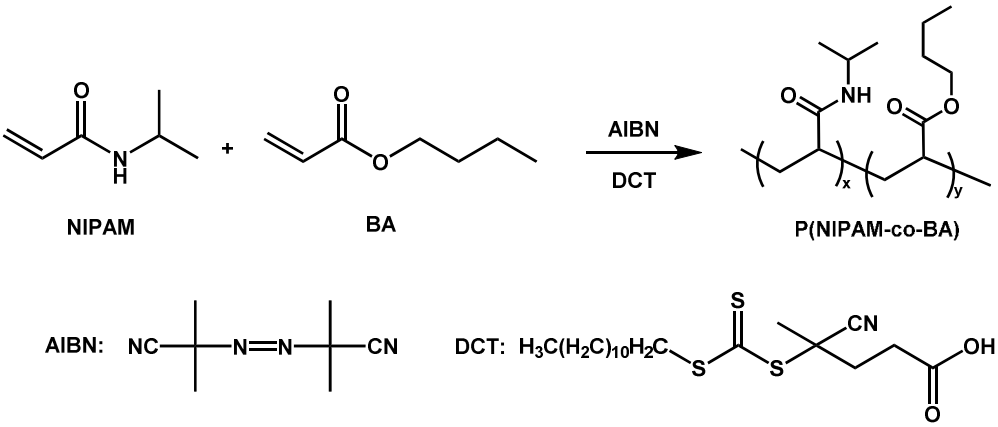

Scheme 1. Synthesis of poly(*N*-isopropylacrylamide-co-butyl acrylate) by RAFT polymerization.

The thermal phase transition of the copolymer was first determined by dynamic light scattering (DLS) in dilute aqueous solution with a polymer concentration of 5 mg mL^{-1}. The lower critical solution temperatures (LCST) or cloud point was taken as the crossing point of the initial slope of the scattering curve vs. the slope of the scattering curve in the middle of the transition (Table 1).[16] For pNIPAM, the light scattering intensity sharply increased in a narrow temperature range, which allowed a precise definition of LCST in the vicinity of 30.5°C. Increased BA content depressed the LCST and caused a marked broadening of the transition. While there was no significant Mw dependence of LCST, an increase in Mw caused a larger particle size of the associated globules formed beyond LCST in DLS measurements.[19] Presumably, the polymer transition was largely controlled by intra-polymer associations in diluted solutions, and therefore the hydrophilic/hydrophobic ratio of the copolymers are a main determinant of their LCST.[20]

Table 1. Characteristics of the synthesized p(NIPAM-co-BA) copolymers

Polymer	$\frac{[BA]}{[NIPAM]}$ [a]	$\frac{[DCT]}{[NIPAM]}$	Yield (%)	Mn [b] (g mol^{-1})	Mw [b] (g mol^{-1})	Đ [b]	LCST[c] (°C)	T_{gel}[d] (°C)
P_{10}(12K)	0.1	0.0076	88	11700	14800	1.26	12	19.2
P_0(16K)	0	0.0038	93	15800	19600	1.24	31	-
P_5(19K)	0.05	0.0038	90	19400	23600	1.22	23	22.5
P_{10}(21K)	0.1	0.0038	93	20700	25000	1.21	13	16.9
P_0(20K)	0	0.0025	95	20500	28100	1.38	31	-
P_5(24K)	0.05	0.0025	96	23500	29600	1.26	23	23.2
P_{10}(29K)	0.1	0.0025	97	29200	33700	1.16	13	14.7
P_0(25K)	0	0.0019	97	24700	33600	1.36	31	-
P_5(31K)	0.05	0.0019	96	30600	40300	1.32	24	23.4
P_{10}(33K)	0.1	0.0019	98	32800	39500	1.20	12	13.0

[a] [DCT]: [AIBN]=5:1. [b] Determined by GPC in THF using polystyrene standards. [c] Determined by DLS measurement of 5 mg mL^{-1} aqueous polymer solution. [d] Determined by oscillatory heating ramp of 30 w/w% aqueous polymer solution.

Phase Transitions

Temperature dependent phase transitions of aqueous solution of p(NIPAM-co-BA) in the 5-30 w/w% range were studied and showed a range of fluid and solid phases, Figure 1a. The gel phases were identified by gently tilting the vials; if no fluidity was visually observed on tilting after 1 min, the sample was determined to be in a gel phase. Phase diagrams were constructed illustrating the phase behavior as a function of concentration and temperature, *e.g.* Figure 1b-e. The polymers were dissolved in aqueous solution at the low temperature (typically below 10°C), forming a homogenous and transparent solution (TS phase). As temperature increased, the polymers showed different phases depending on three factors: concentration, Mw and BA: NIPAM ratio. All of the P_0 solutions became opaque, but remained freely mobile (OS phase) as the temperature was raised from 5°C to 40°C, which is the typical demixing of aqueous pNIPAM solution upon heating (inset in Figure 1a). A similar transition from TS→OS was observed for P_5 and P_{10} copolymers at concentrations below 10% except P_{10}(33K). With increased concentration, the P_5 and P_{10} solutions lost fluidity but remained transparent as the temperature

was raised, forming a transparent gel (TG) phase. The TG phase is stable over long periods for the P_{10} copolymers (*vide infra*), while those formed with P_5 copolymers, specifically P_5(24K) and P_5(31K), flow after standing for roughly 1 hour. The temperature range over which the TG is visible is broadened with increased Mw for P_{10} copolymers (Figure 1b-e). For a specific polymer, the TG phase at high concentrations is formed at a temperature lower than the temperature where the OS phase is first observed for that polymer at low concentrations, indicating that the gels form while pNIPAM is still partially hydrated.[21] The balance between the inter- and intra-polymer interactions should account for the gelation behavior. Hydrophobic microdomains form between the desolvated NIPAM units and the butyl groups in the polymer chains upon heating, and are stabilized by increased BA density. These local microdomains form faster than the formation of the collapsed polymer aggregates, and serve as the physical cross-linkers of the surrounded hydrophilic pNIPAM segments when both the critical Mw and concentration are reached (inset in Figure 1a). An interconnected network hydrogel is formed, allowing TG to precede OS phase.

All of the polymers ultimately formed the OS or dehydrated gel (DG) phase upon heating. P_{10} samples form an opaque gel (OG) phase before the DG phase is observed, *i.e.* TS$\rightarrow$TG$\rightarrow$OG$\rightarrow$DG (Figure 1c-e). An OG phase was also observed for dilute P_{10} samples undergoing TS$\rightarrow$OS transition without the formation of the TG phase. The appearance of the OG phase above the LCST is most likely caused by micelle packing of the collapsed polymer chains.[5] As temperature is increased, the polymer gels undergo macrophase separation, with volume shrinkage by expelling water, and form the final DG phase .

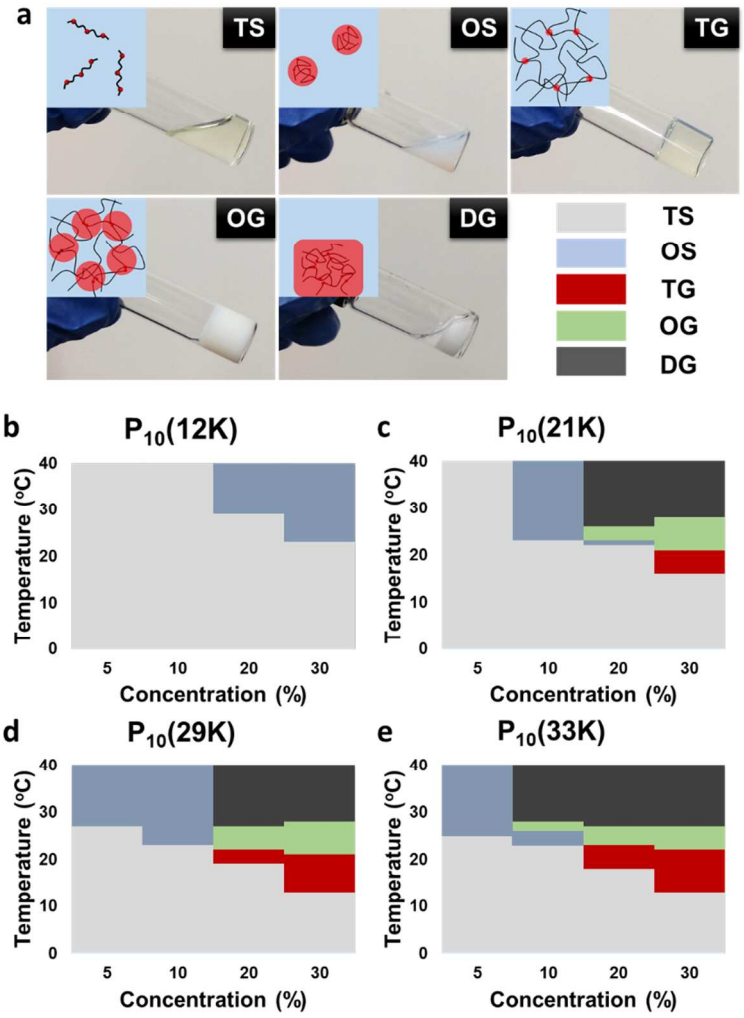

Figure 1. (a) Photograph of the typical phase states during the sol-gel transition of p(NIPAM-co-BA) in aqueous solution. TS: transparent solution phase; OS: opaque solution phase; TG: transparent gel phase; OG: opaque gel phase; DG: dehydrated gel phase. A proposed schematic of the polymer conformational change is given in the inset of each phase state, highlighting the hydrophobic domain (red) and hydrophilic polymer segments (black) in aqueous environment (blue). (b-e) Phase diagram of aqueous p(NIPAM-co-BA) solutions with different molecular weights. The polymers were synthesized at a fixed BA: NIPAM feeding molar ratio of 10:100.

The phase diagram of p(NIPAM-co-BA) shows a full map of its evolution with temperature change, and the dependence on hydrophobic ratio, Mw and concentration. Separate phase transition has been reported for other amphiphilic pNIPAM,[13, 14, 22] but none has found the transition of both OS→OG and TG→OG combined in one copolymer. Particularly, the appearance of transparent gel phase, which is usually observed in the phase transition of block copolymer like PLGA-PEG-PLGA,[5, 23] underscores the importance of precise polymer design. The polymer topology also plays a vital role in directing its phase transition, and a block copolymer pNIPAM-b-pBA with the same composition as the random copolymer showed limited solubility in aqueous solution, and the thermal transition occurred at the same range with pNIPAM (data not shown), which is contrary to the generally accepted view in designing thermo-gelling polymers.[5, 7] Tunable random copolymers prepared from a thermo-responsive monomer and hydrophobic comonomers would provide a new family of thermosensitive hydrogels, and the reversible sol-gel transition can be potentially used for injectable materials with unique applications in biomedical field.

Rheological Analysis

Dynamic modulus measurements were employed to study phase transitions, which allows for the precise determination of the response of each material to an oscillatory force (stress) or deformation (strain). The viscoelastic properties of materials can be evaluated by measurements of storage modulus G' (elastic behavior), loss modulus G" (viscous behavior), and loss tangent (the ratio of G" to G', tan δ=G"/G'). An oscillation temperature ramp was first applied within the Linear Viscoelastic Region (LVR) of the polymer, where the modulus is independent of the amplitude of the deformation. A typical curve of the polymer that exhibited TS→TG→OG→DG transitions was shown as Figure 2a, and it could be readily partitioned into the different phases.

At low temperatures, the polymers behaved as a viscous liquid (G" > G'). Both the storage and loss moduli increased with temperature as the result of enhanced interpolymer interaction, and the gelation temperature (T_{gel}) was determined as the crossing point of G' and G" (G'=G", tan δ=1),[14] which shows the starting point where the system turns into an elastic network from a viscous fluid. An equilibrium modulus was not observed as temperature changed, and a more elastic gel was formed as evidenced by the steady increase of storage modulus compared with loss modulus. Following the minimum of loss tangent, a sharp increase of moduli occurred, with gel strength improved by more than two orders of magnitude, indicative of the aggregation of collapsed pNIPAM chains, and a second crossing point of G' and G" was also included in this region. The fall of the moduli after the maximum values corresponded to the macroscopic phase separation of the systems.

The temperature dependence of G' and G" is controlled by the polymer's BA: NIPAM ratio, Mw and concentration. The profiles of polymer modulus with the occurrence of G' ≥ G" were summarized in Figure 2b for 30% solutions and Figure S5 for 20% solutions. For P_{10} copolymers, the gel region became broader with both increased Mw and concentration. P_{10}(12K) at 20% and 30% and P_{10}(21K) at 20% showed G' ≥ G", however, the region occurred within a narrow temperature range and without the obvious characteristic of elastic gel formation. These observations are consistent with the missing TG phase in their phase diagrams. In contrast to the similar LCST values determined by DLS, T_{gel} for the P_{10} copolymers showed a decreasing trend with increased Mw, which confirms the importance of interpolymer interaction in directing gel formation. No clear relationship can be established for the P_5 copolymers, with little increase or even decrease of modulus during gel formation, and T_{gel} was not significantly affected by Mw.

For the other polymers, which did not show a TG phase, a loss tangent higher than 1 (G”>G’) was observed throughout the oscillation temperature ramp.

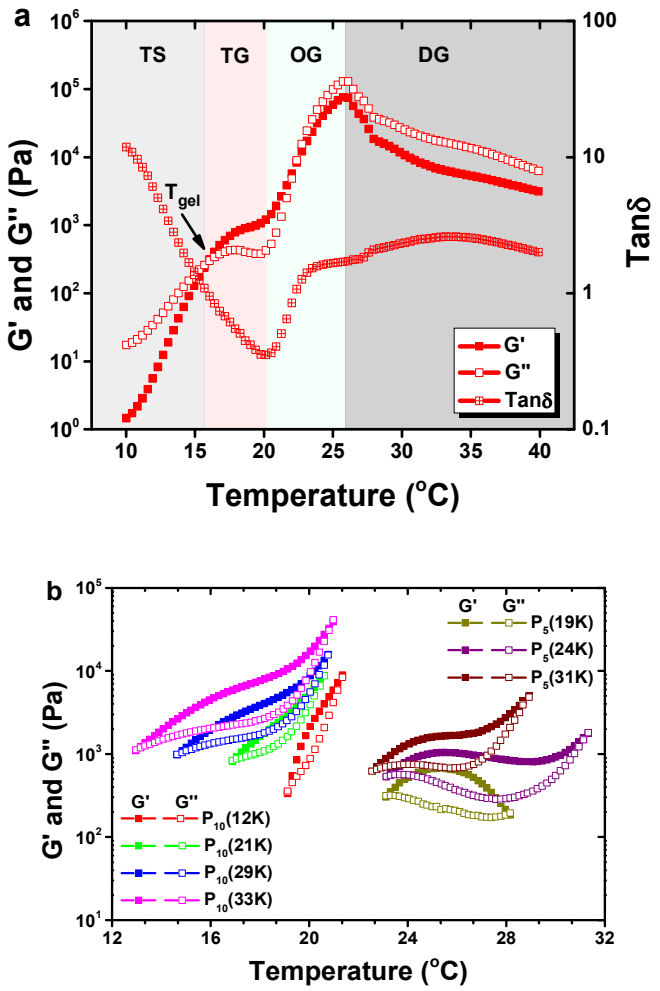

Figure 2. (a) Oscillatory temperature ramp of 20 w/w% aqueous P_{10}(33K) solution. The cross-over point of storage (G’) and loss (G’’) modulus is defined as the gelation temperature (T_{gel}). The temperature ramp curve was segmented into different phase states by visual observation of the samples at the same heating rate as the rheological analysis. (b) Summary of the temperature ramp curves of 30 w/w% aqueous p(NIPAM-co-BA) solutions at the regions with G’ ≥ G’’. Measurements were performed at a constant strain of 1% and frequency of 6.3 rad s^{-1}.

G' > G" indicates a prevalently elastic state for a material, and the properties of polymers within the closed loop of G' and G" (the gel region) would be of great interest for potential biomedical application. An extensive strain-amplitude sweep study was conducted on 20% solutions of P_{10}(33K) within its gel region (Figure 3a). It was revealed that the extent of LVR strongly depended on temperature. An increased plateau modulus G' was observed upon heating, which reflected a rise in rigidity caused by a growing density of hydrophobic cross-links.[24] However, while the hydrogel structure withstood up to 100% strain at 16 °C, a breakdown of the gel structure was observed around 1.7% strain at 21 °C. Accordingly, the loss tangent dropped first and then rose with ascending temperature (inset Figure 3a), which is a similar trend to the temperature ramp curve of Figure 2a. However, the tan δ >1 beyond 20 °C indicated the polymer reached OG phase under isothermal condition, which was not distinguished during a consecutive heating process. Continuing aggregation of butyl groups and desolvated NIPAM units caused micro-phase separation during OG phase, such that there were no clear boundaries between OG and DG phases. The extended LVR at TG phases suggested that the gel formed was elastic and could resist greater deformations than its OG phases. An optimal gel performance can be achieved with moderate stiffness (~10^3 Pa) and minimum loss tangent while accompanied by little loss of LVR.

The time dependence of its viscoelastic properties was further evaluated by varying the frequency of the applied strain in the linear viscoelastic regime for P_{10}(33K) at the concentration of 20% (Figure 3b). The gels formed at different temperatures all exhibited frequency-dependent dynamic moduli and a loss tangent above 0.1 (Figure S6), indicating the temporary nature of hydrophobic associations.[9] At low frequencies G" was greater than G' in most cases and therefore the system was predominantly viscous (tan δ > 1), while at higher frequencies the

situation is reversed with G' larger than G" and therefore elastic, solid-like behavior dominated (tan $\delta < 1$). The frequency at which G' and G" cross (tan $\delta = 1$) could be used to calculate the characteristic relaxation time of the network, $\tau \sim 1/\omega_c$.[25] An increasing relaxation time was observed from 16 °C to 19 °C, which was ascribed to the occurrence of a reversible network. A power law scaling of G'(ω) and G"(ω) showed that the power law exponent significantly deviated from the typical value of a viscoelastic fluid (G'~ ω^2 and G"~ ω) in the low-frequency window ($\omega\tau < 1$). In the high-frequency range ($\omega\tau > 1$), G' increased with frequency, while G" was nearly constant, which has been observed for other gels based on thermoresponsive block copolymers.[26, 27] At 19 °C, the gel displayed the highest degree of elasticity, with G' only weakly dependent on frequency ($G' \sim \omega^{0.35}$) and greater than G" over the entire frequency range, a behavior typical for chemical or strongly interacting physical gels.[28] Further increase of temperature shifted the ω_c to higher frequency, and G" dominated over G' within the frequency range studied at 21 °C. The scaling behaviors of the dynamic moduli with $G' \sim \omega^{2.29}$ and $G'' \sim \omega^{1.24}$ indicated that the gels were not actually a real gel at this temperature, and behaved as a viscoelastic fluid.

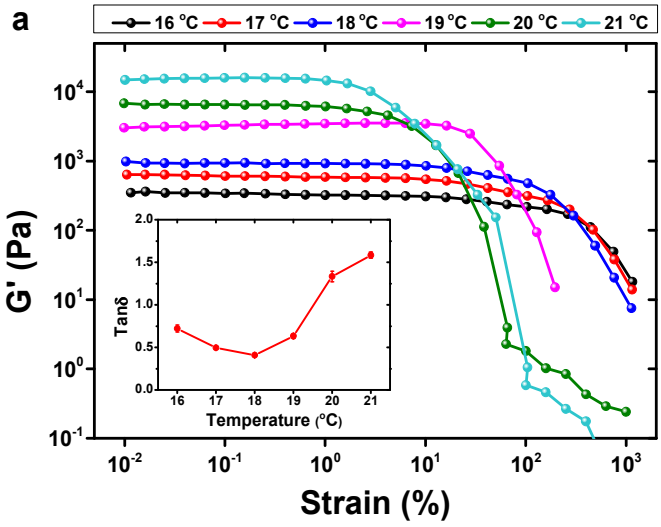

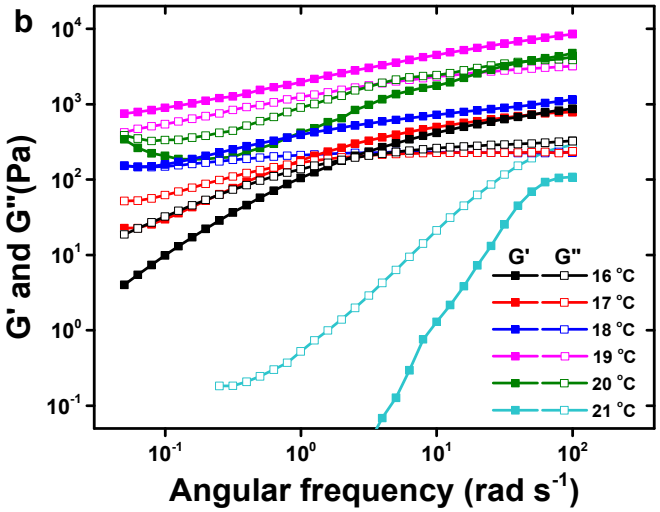

	16 °C	17 °C	18 °C	19 °C	20 °C	21 °C
ω_c (rad/s)	2.13	0.83	0.05	-	47.2	-
G'(ω)	1.14/0.31	0.81/0.2	-/0.37	-/0.35	0.66/-	2.29/-
G''(ω)	0.72/0.09	0.47/0.01	-/0.13	-/0.35	0.57/-	1.24/-

Figure 3. (a) Dynamic strain sweep of 20 w/w% aqueous P_{10}(33K) solution at the gel region determined by the oscillatory temperature ramp. The inset shows the loss tangent (G''/G') change with temperature in the linear viscoelastic region (LVR). Measurements were performed at a constant frequency of 6.3 rad s^{-1}. (b) Frequency sweep of 20 w/w% aqueous P_{10}(33K) solution at the gel region determined by the oscillatory temperature ramp. Measurements were performed at a constant strain of 0.5%. Both the G' and G'' were fitted to a power-law rheology model before and after the frequency where the modulus crossover (ω_c), and the power law exponents were listed together with ω_c in the table below the panel.

Reversibility and stability

A stable hydrogel formed within a controllable temperature window is highly attractive for serving as an injectable thermosensitive material, which motivated us to further investigate the

gel properties. When the temperature was cycled between TS and TG phases, the hydrogel showed a reversible sol-gel transition, as shown in Figure 4a. A stable gel formed instantaneously upon temperature jumping from 5 to 18 °C, and the elastic modulus reached a plateau within 1 min. The gel disintegrated rapidly upon cooling to 5 °C, regained its liquid behavior, and both the elastic and loss moduli returned to their initial values immediately. The gel displayed complete recovery of rheological properties after three heating/cooling cycles. No plateau modulus was detected when the temperature was shifted to OG or DG phase from TS phase (Figure S7). The demixing of the gels caused a greater G" value than G'. Within the time scale studied, the direct cooling does not restore its initial rheological properties in the TS phase, and the deviations from its original properties became even larger after repeated heating/cooling cycles between the TS and OG/DG phases.

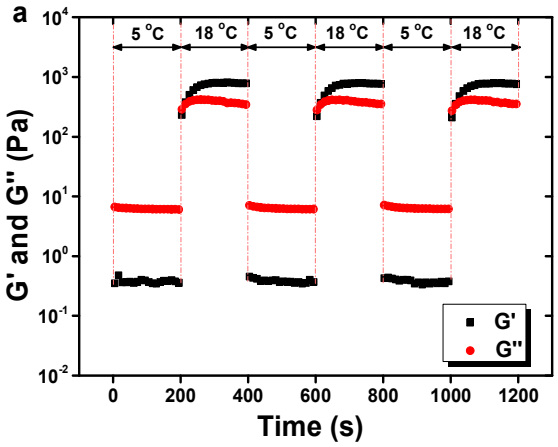

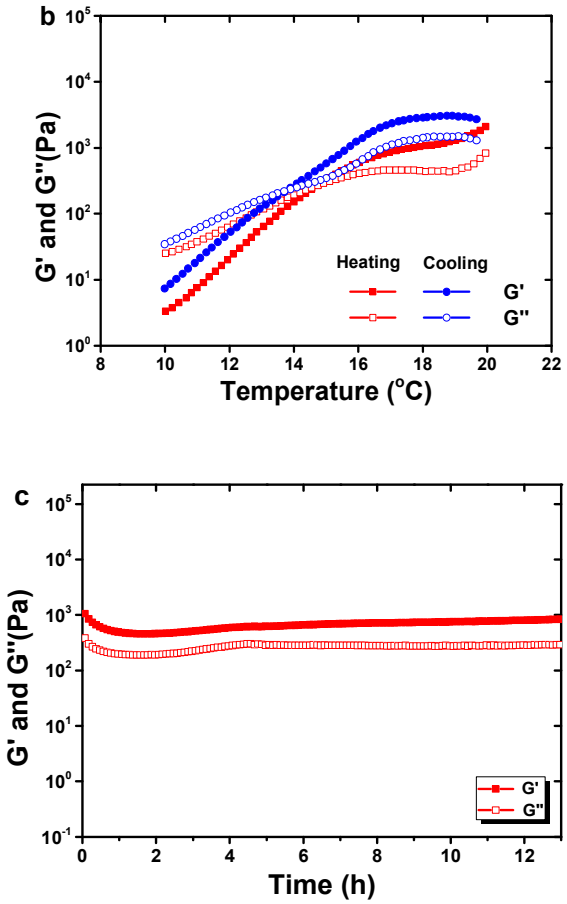

Figure 4. Thermo-reversibility and stability of p(NIPAM-co-BA) at TG phase. (a) Rheological reversibility between 5 °C (TS phase) and 18 °C (TG phase). (b) Rheological hysteresis curves in a heating and cooling cycle between 10 °C (TS) and 18 °C (TG). (c) Long-term rheological stability in an oscillatory time sweep at 18 °C (TG). The aqueous polymer solution was made of P_{10}(33K) at the concentration of 20 w/w%.

Hysteresis is common in coil-globule-coil transition of pNIPAM and thermally reversible gelation of block copolymers,[29, 30] due to the hindrance of polymer rehydration by the additional interactions formed in the collapsed state (e.g., hydrogen bonds). Heating and cooling ramps were applied successively between the different phases, and the rheological hysteresis curves is illustrated in Figure 4b (TS↔TG) and Figure S8 (TS↔OG and TS↔DG). The crossover point

of G' and G" cooling curves corresponds to the gel melting temperature (T_m).[29] The gel was highly reversible between TS and TG phases, showing a hysteresis of less than 1 °C between the T_m and T_{gel} at the given heating/cooling cycles. In contrast, strong hysteresis was observed when the polymer was driven into the OG phase, with large deviation of cooling diagrams from its heating counterpart. The situation was further aggravated for the DG phase, as marked phase separation took place at this stage.

The temporal stability of the gel properties was also studied. As showed in Figure 4c, the gel was quite stable at 18 °C. During an observation period of 12 hours, we observed almost no change of G' and G". However, marked change was observed for the polymer in the OG and DG phases (Figure S9), which was a result of the continuous phase separation and increased stiffness of its polymer rich phase.

Self-healing

Considering the reversible and dynamic nature of hydrophobic interactions, the hydrogel network is expected to exhibit self-healing capacity.[8, 9] A strain amplitude sweep at 18 °C has showed the network destruction occurred above the strain of 100% for the gel formed of P_{10}(33K)@20% (Figure 3a). The rheological response of the same gel was studied at alternate step strains within and out of its linear viscoelastic region. As shown in Figure 5a, the gel was initially elastic at a small strain of 1%, and G' and G" were constant against time. When the oscillation strain was shifted to 1000%, the gel immediately failed with dramatic decrease in both G' and G", and showed a quasi-liquid behavior (G'< G"). Low strain of 1% was reapplied after the gels were destroyed, and the flowable system rapidly recovered to form a gel phase (G'>G"), with both G' and G" recovered quickly to their initial levels. The failure-recovery cycle was repeated four times without any distinct change of rheological properties.

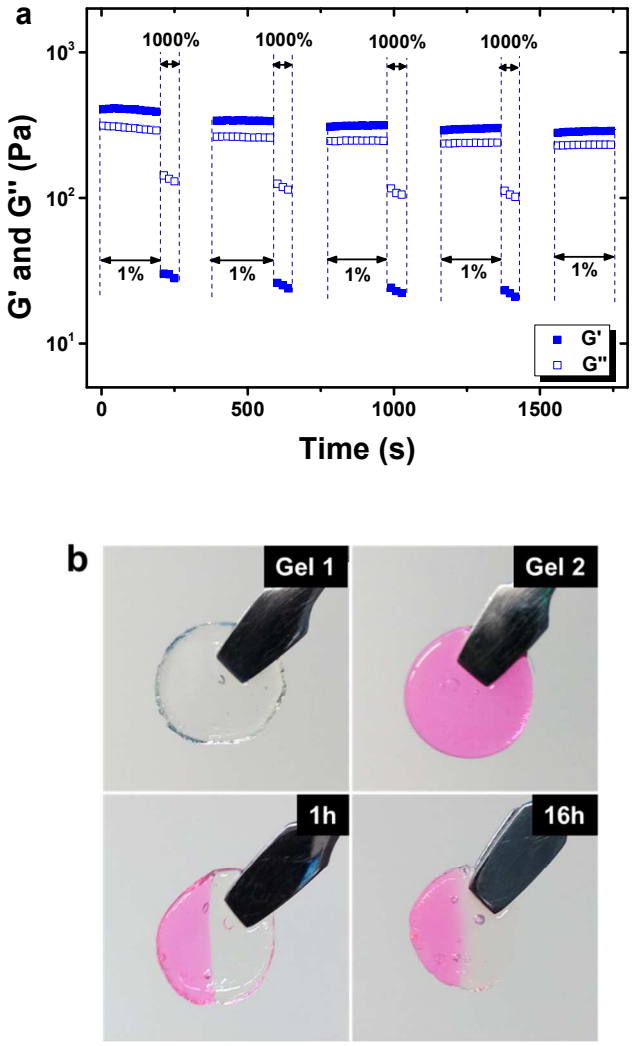

Figure 5. (a) Storage (G') and loss modulus (G'') responsiveness of the p(NIPAM-co-BA) hydrogel when alternate step strain switched from small strain (γ = 1%) to large strain (γ = 1000%) at a fixed angular frequency (6.3 rad s^{-1}) and constant temperature (18 °C). The polymer gel was made of P_{10}(33K) at the concentration of 20 w/w%. (b) Photographs showing the self-healing process of p(NIPAM-co-BA) hydrogel at constant temperature (18 °C). One piece of the gels was stained with rhodamine B (red dye) to facilitate visualization.

The self-healing capacity was also confirmed by visual observation of the healing of two cut hydrogels (Figure 5b). Two hydrogel sheets were prepared at 18 °C with one stained with

rhodamine B. After cutting the gels into two pieces, the dyed and non-dyed pieces were brought together by simply joining the fresh-cut surface. These pieces merged into a single sheet in 1 hour. The healing and dye diffusion proceeded with time, and no obvious border could be observed after 16 hours. The joint was strong enough to allow for stretching without tearing through the previous fracture surface. The dynamic nature of hydrophobic cross-links allowed the continuous movement and re-association of the polymer chains, favoring the reconstruction of the hydrogel network and the consequent diffusion of the dye through the rupture areas.[31] The self-healing properties of p(NIPAM-co-BA) could be further translated into auto-healing behaviors of the polymers with different molecular weights, as long as they exhibited the same temperature range of gel phase determined by phase diagram and rheological analysis (Figure S10).

CONCLUSIONS

The solution properties of p(NIPAM-co-BA) polymers were studied in dilute and semidilute ranges (5 – 30 wt%). Phase diagram and rheological analysis established a full map of the phase behaviors induced by the evolution of polymer dynamics in this copolymer system. A unique physical hydrogel can be produced by the fine tunability of Mw, BA: NIPAM ratio, and aqueous concentration, which was stabilized by the hydrophobic domains of butyl group and desolvated NIPAM units. The gel properties were strongly dependent on temperature, and it was proved to be highly elastic, stable and reversible within a given temperature range. Self-healing capability against external disruption was also demonstrated due to the dynamic nature of hydrophobic association. The on-demand responsive properties will be highly desirable for injectable in situ forming hydrogel materials.

ACKNOWLEDGEMENTS

The authors thank Dr. Peter Djurovich and Roby Menefee for helpful discussion and constructive advice. Financial support is gratefully acknowledged from the Department of Defense through the United States Army Telemedicine and Advanced Technology Research Center (TATRC) vision research program, grant #: JW150025.

ASSOCIATED CONTENT

Supporting Information. FTIR, NMR and GPC characterization of p(NIPAM-co-BA), DLS results of p(NIPAM-co-BA) solutions, additional figures of phase diagram, rheological analysis and self-healing process.

REFERENCES

1. Y. S. Zhang and A. Khademhosseini, *Science*, 2017, **356**.
2. M. Guo, L. M. Pitet, H. M. Wyss, M. Vos, P. Y. W. Dankers and E. W. Meijer, *Journal of the American Chemical Society*, 2014, **136**, 6969-6977.
3. B. Li, K. Ren, Y. Wang, Y. Qi, X. Chen and Y. Huang, *ACS Applied Materials & Interfaces*, 2016, **8**, 30788-30796.
4. E. E. Meyer, K. J. Rosenberg and J. Israelachvili, *Proceedings of the National Academy of Sciences*, 2006, **103**, 15739-15746.
5. L. Yu and J. Ding, *Chemical Society Reviews*, 2008, **37**, 1473-1481.
6. B. Jeong, S. W. Kim and Y. H. Bae, *Advanced Drug Delivery Reviews*, 2002, **54**, 37-51.
7. A. P. Constantinou and T. K. Georgiou, *European Polymer Journal*, 2016, **78**, 366-375.
8. D. C. Tuncaboylu, M. Sari, W. Oppermann and O. Okay, *Macromolecules*, 2011, **44**, 4997-5005.
9. U. Gulyuz and O. Okay, *European Polymer Journal*, 2015, **72**, 12-22.
10. A. Halperin, M. Kröger and F. M. Winnik, *Angewandte Chemie International Edition*, 2015, **54**, 15342-15367.
11. F. Zeng, X. Zheng and Z. Tong, *Polymer*, 1998, **39**, 1249-1251.

12. S. Nakano, T. Ogiso, R. Kita, N. Shinyashiki, S. Yagihara, M. Yoneyama and Y. Katsumoto, *The Journal of Chemical Physics*, 2011, **135**, 114903.

13. Y. Lu, Y. Han, J. Liang, H. Meng, F. Han, X. Wang and C. Li, *Polymer Chemistry*, 2011, **2**, 1866-1871.

14. V. Wintgens and C. Amiel, *Macromolecular Chemistry and Physics*, 2008, **209**, 1553-1563.

15. X. Yang, H. Y. Lee and J.-C. Kim, *Journal of Applied Polymer Science*, 2011, **120**, 2346-2353.

16. Y. Zhang, S. Furyk, D. E. Bergbreiter and P. S. Cremer, *Journal of the American Chemical Society*, 2005, **127**, 14505-14510.

17. F. Ganachaud, M. J. Monteiro, R. G. Gilbert, M.-A. Dourges, S. H. Thang and E. Rizzardo, *Macromolecules*, 2000, **33**, 6738-6745.

18. G. Moad, E. Rizzardo and S. H. Thang, *Australian Journal of Chemistry*, 2005, **58**, 379-410.

19. A. J. Convertine, B. S. Lokitz, Y. Vasileva, L. J. Myrick, C. W. Scales, A. B. Lowe and C. L. McCormick, *Macromolecules*, 2006, **39**, 1724-1730.

20. H. Ringsdorf, J. Venzmer and F. M. Winnik, *Macromolecules*, 1991, **24**, 1678-1686.

21. E. Schoolaert, P. Ryckx, J. Geltmeyer, S. Maji, P. H. M. Van Steenberge, D. R. D'Hooge, R. Hoogenboom and K. De Clerck, *ACS Applied Materials & Interfaces*, 2017, DOI: 10.1021/acsami.7b05074.

22. C. K. Han and Y. H. Bae, *Polymer*, 1998, **39**, 2809-2814.

23. S. Aoshima and S. Sugihara, *Journal of Polymer Science Part A: Polymer Chemistry*, 2000, **38**, 3962-3965.

24. S. Himmelein, V. Lewe, M. C. A. Stuart and B. J. Ravoo, *Chemical Science*, 2014, **5**, 1054-1058.

25. C. R. López-Barrón, R. Chen, N. J. Wagner and P. J. Beltramo, *Macromolecules*, 2016, **49**, 5179-5189.

26. Y. He and T. P. Lodge, *Chemical Communications*, 2007, DOI: 10.1039/B704490A, 2732-2734.

27. D. Cohn, A. Sosnik and S. Garty, *Biomacromolecules*, 2005, **6**, 1168-1175.

28. K. A. Aamer, H. Sardinha, S. R. Bhatia and G. N. Tew, *Biomaterials*, 2004, **25**, 1087-1093.

29. K. J. Krzyminski, M. Jasionowski and A. Gutowska, *Polymer International*, 2008, **57**, 592-604.

30. L. Yu, H. Zhang and J. Ding, *Angewandte Chemie International Edition*, 2006, **45**, 2232-2235.

31. A. Pettignano, M. Haring, L. Bernardi, N. Tanchoux, F. Quignard and D. Diaz Diaz, *Materials Chemistry Frontiers*, 2017, **1**, 73-79.